BPS Dendroscopy on Local $\mathbb{P}^2$

Boris Pioline

Geometry and QFT, 20/10/2022

Based on [2210.10712] with Pierrick Bousseau, Pierre Descombes and Bruno Le Floch

My amazing co-authors

  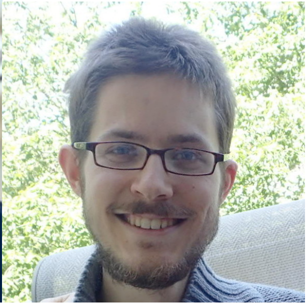

Introduction

- In type IIA string theory compactified on a Calabi-Yau threefold X, the BPS spectrum consists of bound states of D6-D4-D2-D0 branes, with charge $\gamma \in H_{\rm even}(X, \mathbb{Q})$.

Introduction

- In type IIA string theory compactified on a Calabi-Yau threefold X, the BPS spectrum consists of bound states of D6-D4-D2-D0 branes, with charge $\gamma \in H_{\rm even}(X, \mathbb{Q})$.
- The BPS index $\Omega_z(\gamma)$ counts states saturating the BPS bound $M(\gamma) \geq |Z(\gamma)|$, where $Z \in \mathrm{Hom}(\Gamma, \mathbb{C})$ depends on the complexified Kähler moduli $z \in \mathcal{M}_K$.

Introduction

- In type IIA string theory compactified on a Calabi-Yau threefold X, the BPS spectrum consists of bound states of D6-D4-D2-D0 branes, with charge $\gamma \in H_{\rm even}(X, \mathbb{Q})$.
- The BPS index $\Omega_z(\gamma)$ counts states saturating the BPS bound $M(\gamma) \geq |Z(\gamma)|$, where $Z \in \mathrm{Hom}(\Gamma, \mathbb{C})$ depends on the complexified Kähler moduli $z \in \mathcal{M}_K$.
- Mathematically, the Donaldson-Thomas invariant $\Omega_z(\gamma)$ counts stable objects with $\mathrm{ch}\, E = \gamma$ in the derived category of coherent sheaves $\mathcal{C} = D^b\mathrm{Coh}(X)$.

Introduction

- $\Omega_z(\gamma)$ is locally constant on $\mathcal{M}_K$, but can jump across real codimension one walls of marginal stability $\mathcal{W}(\gamma_L, \gamma_R) \subset \mathcal{M}_K$, where the phases of the central charges $Z(\gamma_L)$ and $Z(\gamma_R)$ with $\gamma = m_L\gamma_L + m_R\gamma_R$ become aligned *[Kontsevich Soibelman'08, Joyce Song'08]*

Introduction

- $\Omega_z(\gamma)$ is locally constant on $\mathcal{M}_K$, but can jump across real codimension one walls of marginal stability $\mathcal{W}(\gamma_L, \gamma_R) \subset \mathcal{M}_K$, where the phases of the central charges $Z(\gamma_L)$ and $Z(\gamma_R)$ with $\gamma = m_L\gamma_L + m_R\gamma_R$ become aligned *[Kontsevich Soibelman'08, Joyce Song'08]*
- Physically, multi-centered black hole solutions with charges $\gamma_i = m_{L,i}\gamma_L + m_{R,i}\gamma_R$ (dis)appear across the wall *[Denef Moore '07, ..., Manschot BP Sen '11]*.

Introduction

- $\Omega_z(\gamma)$ is locally constant on $\mathcal{M}_K$, but can jump across real codimension one walls of marginal stability $\mathcal{W}(\gamma_L, \gamma_R) \subset \mathcal{M}_K$, where the phases of the central charges $Z(\gamma_L)$ and $Z(\gamma_R)$ with $\gamma = m_L\gamma_L + m_R\gamma_R$ become aligned *[Kontsevich Soibelman'08, Joyce Song'08]*
- Physically, multi-centered black hole solutions with charges $\gamma_i = m_{L,i}\gamma_L + m_{R,i}\gamma_R$ (dis)appear across the wall *[Denef Moore '07, ..., Manschot BP Sen '11]*.
- Most of these multi-centered bound states are expected to be absent at the attractor point $z_\star(\gamma)$, defined as the endpoint of the attractor flow *[Ferrara Kallosh Strominger'95]*

$$\mathrm{AF}_\gamma : \quad r^2 \frac{\mathrm{d}z^a}{\mathrm{d}r} = -g^{a\bar{b}}\partial_{\bar{b}}|Z_z(\gamma)|^2$$

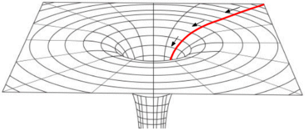

The Split Attractor Flow Conjecture

- Since $Z_z(\gamma)$ decreases along the flow, $z_\star(\gamma)$ is either a local minimum of $|Z_z(\gamma)| > 0$, or a conifold point if $Z_{z_\star(\gamma)}(\gamma) = 0$. We define the attractor invariant as $\Omega_\star(\gamma) = \Omega_{z_\star(\gamma)}(\gamma)$.

The Split Attractor Flow Conjecture

- Since $Z_z(\gamma)$ decreases along the flow, $z_\star(\gamma)$ is either a local minimum of $|Z_z(\gamma)| > 0$, or a conifold point if $Z_{z_\star(\gamma)}(\gamma) = 0$. We define the attractor invariant as $\Omega_\star(\gamma) = \Omega_{z_\star(\gamma)}(\gamma)$.
- Starting from $z \in \mathcal{M}_K$, following AF_γ and recursively applying the WCF formula at whenever the flow crosses a wall of marginal stability, one can in principle express $\Omega_z(\gamma)$ in terms of attractor invariants.

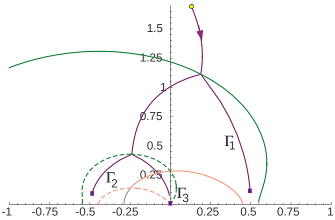

Denef Moore'07

The Split Attractor Flow Conjecture (SFAC)

- In terms of the rational DT invariants

$$\bar{\Omega}_z(\gamma) := \sum_{k|\gamma} \frac{y-1/y}{k(y^k-y^{-k})} \Omega_z(\gamma/k)_{y\to y^k}$$

the result takes the form

$$\bar{\Omega}_z(\gamma) = \sum_{\gamma=\sum \gamma_i} \frac{g_z(\{\gamma_i\})}{\mathrm{Aut}(\{\gamma_i\})} \prod_i \bar{\Omega}_\star(\gamma_i)$$

where $g_z(\{\gamma_i\})$ is a sum over 'attractor flow trees'.

The Split Attractor Flow Conjecture (SFAC)

- In terms of the rational DT invariants

$$\bar{\Omega}_z(\gamma) := \sum_{k|\gamma} \frac{y-1/y}{k(y^k-y^{-k})} \Omega_z(\gamma/k)_{y\to y^k}$$

the result takes the form

$$\bar{\Omega}_z(\gamma) = \sum_{\gamma=\sum\gamma_i} \frac{g_z(\{\gamma_i\})}{\mathrm{Aut}(\{\gamma_i\})} \prod_i \bar{\Omega}_\star(\gamma_i)$$

where $g_z(\{\gamma_i\})$ is a sum over 'attractor flow trees'.

- The Split Attractor Flow Conjecture *[Denef'00, Denef Moore'07]* is the statement that only a finite number of decompositions $\gamma = \sum \gamma_i$ contribute to the index $\bar{\Omega}_z(\gamma)$.

The Split Attractor Flow Conjecture

- The problem is that one does not know a priori which constituents γ_i can contribute, except for the constraints

$$\sum_i \gamma_i = \gamma \;, \quad \sum_i |Z_{z_\star(\gamma_i)}(\gamma_i)| < |Z_z(\gamma)|$$

The Split Attractor Flow Conjecture

- The problem is that one does not know a priori which constituents γ_i can contribute, except for the constraints

$$\sum_i \gamma_i = \gamma \,, \quad \sum_i |Z_{z_\star(\gamma_i)}(\gamma_i)| < |Z_z(\gamma)|$$

- In particular, there can be cancellations between D-branes and anti-D-branes, and contribution from conifold states which are massless at their attractor point are hard to bound.

The Split Attractor Flow Conjecture

- The problem is that one does not know a priori which constituents γ_i can contribute, except for the constraints

$$\sum_i \gamma_i = \gamma \; , \quad \sum_i |Z_{z_\star(\gamma_i)}(\gamma_i)| < |Z_z(\gamma)|$$

- In particular, there can be cancellations between D-branes and anti-D-branes, and contribution from conifold states which are massless at their attractor point are hard to bound.
- Even if SAFC holds, one still has to compute the attractor indices $\Omega_\star(\gamma)$, a tall order for regular attractor points.

The Split Attractor Flow Conjecture

- The problem is that one does not know a priori which constituents γ_i can contribute, except for the constraints

$$\sum_i \gamma_i = \gamma \,, \quad \sum_i |Z_{z_\star(\gamma_i)}(\gamma_i)| < |Z_z(\gamma)|$$

- In particular, there can be cancellations between D-branes and anti-D-branes, and contribution from conifold states which are massless at their attractor point are hard to bound.
- Even if SAFC holds, one still has to compute the attractor indices $\Omega_\star(\gamma)$, a tall order for regular attractor points.
- Besides single-centered black holes, $\Omega_\star(\gamma)$ also gets contributions multi-centered scaling solutions. The Coulomb Branch Formula *[Manschot BP Sen'12]* allows to disentangle them, but suffers from same difficulties as SAFC.

Summary

- Our aim is to investigate the Split Attractor Flow Conjecture for one of the simplest examples of CY threefolds, namely $X = K_{\mathbb{P}^2} = \widetilde{\mathbb{C}^3/\mathbb{Z}_3}$ *[Douglas Fiol Romelsberger'00]*.

Summary

- Our aim is to investigate the Split Attractor Flow Conjecture for one of the simplest examples of CY threefolds, namely $X = K_{\mathbb{P}^2} = \widetilde{\mathbb{C}^3/\mathbb{Z}_3}$ *[Douglas Fiol Romelsberger'00]*.
- We show that the only possible constituents are the $\Gamma_1(3)$ images of the D4-brane $\mathcal{O}_{\mathbb{P}^2}$ and anti-D4-brane $\mathcal{O}_{\mathbb{P}^2}[1]$, each carrying attractor index $\Omega_\star(\gamma) = 1$.

Summary

- Our aim is to investigate the Split Attractor Flow Conjecture for one of the simplest examples of CY threefolds, namely $X = K_{\mathbb{P}^2} = \widetilde{\mathbb{C}^3/\mathbb{Z}_3}$ *[Douglas Fiol Romelsberger'00]*.
- We show that the only possible constituents are the $\Gamma_1(3)$ images of the D4-brane $\mathcal{O}_{\mathbb{P}^2}$ and anti-D4-brane $\mathcal{O}_{\mathbb{P}^2}[1]$, each carrying attractor index $\Omega_\star(\gamma) = 1$.
- In particular, in the large volume region the full BPS spectrum arises as bound states of fluxed D4 and anti-D4-brane, with effective bounds on the number and flux of the constituents.

Summary

- Our aim is to investigate the Split Attractor Flow Conjecture for one of the simplest examples of CY threefolds, namely $X = K_{\mathbb{P}^2} = \widetilde{\mathbb{C}^3/\mathbb{Z}_3}$ *[Douglas Fiol Romelsberger'00]*.
- We show that the only possible constituents are the $\Gamma_1(3)$ images of the D4-brane $\mathcal{O}_{\mathbb{P}^2}$ and anti-D4-brane $\mathcal{O}_{\mathbb{P}^2}[1]$, each carrying attractor index $\Omega_\star(\gamma) = 1$.
- In particular, in the large volume region the full BPS spectrum arises as bound states of fluxed D4 and anti-D4-brane, with effective bounds on the number and flux of the constituents.
- A key role is played by scattering diagrams, which provide the correct mathematical framework for the SAFC, at least for local CY threefolds.

Outline

Outline

Kähler moduli space

- By local mirror symmetry, the Kähler moduli space of $X = K_{\mathbb{P}^2}$ is the quotient $X_1(3) = \mathbb{H}/\Gamma_1(3)$ parametrizing elliptic curves with level structure. It admits two cusps LV, C and one orbifold point o.

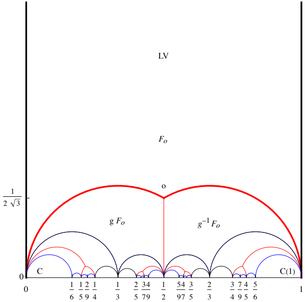

Kähler moduli space

- By local mirror symmetry, the Kähler moduli space of $X = K_{\mathbb{P}^2}$ is the quotient $X_1(3) = \mathbb{H}/\Gamma_1(3)$ parametrizing elliptic curves with level structure. It admits two cusps LV, C and one orbifold point o.

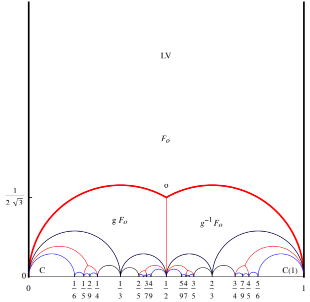

- A BPS state on X is an object E in the derived category $\mathcal{C}$ of compactly supported sheaves on X, with charge $\gamma(E) = \text{ch}(\pi_*(E)) = [r, d, \text{ch}_2] \sim [D4, D2, D0]$

Central charge as Eichler integral

- The central charge $Z_\tau(\gamma)$ is a linear combination

$$Z_\tau(\gamma) = -rT_D(\tau) + dT(\tau) - \mathrm{ch}_2$$

where T_D, T are single-valued functions on $\mathbb{H}$ (but not on $\mathcal{M}_K$). They are periods of a one-form λ with logarithmic singularities on the mirror curve, satisfying a Picard-Fuchs equation of degree 3.

Central charge as Eichler integral

- The central charge $Z_\tau(\gamma)$ is a linear combination

$$Z_\tau(\gamma) = -rT_D(\tau) + dT(\tau) - \mathrm{ch}_2$$

where T_D, T are single-valued functions on $\mathbb{H}$ (but not on $\mathcal{M}_K$). They are periods of a one-form λ with logarithmic singularities on the mirror curve, satisfying a Picard-Fuchs equation of degree 3.

- It turns out that $\partial_\tau \lambda$ is holomorphic, so its periods are proportional to $(1, \tau)$. Integrating along a path from o to τ, one can establish the Eichler-type integral representation

$$\boxed{\begin{pmatrix} T \\ T_D \end{pmatrix} = \begin{pmatrix} 1/2 \\ 1/3 \end{pmatrix} + \int_{\tau_o}^{\tau} \begin{pmatrix} 1 \\ u \end{pmatrix} C(u)\,\mathrm{d}u}$$

where $C(\tau) = \frac{\eta(\tau)^9}{\eta(3\tau)^3}$ is a weight 3 modular form for $\Gamma_1(3)$.

Central charge as Eichler integral

- This provides an computationally efficient analytic continuation of Z_τ throughout $\mathbb{H}$, and gives access to monodromies:

$$\tau \mapsto \frac{a\tau+b}{c\tau+d} \qquad \begin{pmatrix} 1 \\ T \\ T_D \end{pmatrix} \mapsto \begin{pmatrix} 1 & 0 & 0 \\ m & d & c \\ m_D & b & a \end{pmatrix} \cdot \begin{pmatrix} 1 \\ T \\ T_D \end{pmatrix}$$

where (m, m_D) are period integrals of C from τ_o to $\frac{d\tau_o - b}{a - c\tau_o}$.

Central charge as Eichler integral

- This provides an computationally efficient analytic continuation of Z_τ throughout $\mathbb{H}$, and gives access to monodromies:

$$\tau \mapsto \frac{a\tau+b}{c\tau+d} \qquad \begin{pmatrix} 1 \\ T \\ T_D \end{pmatrix} \mapsto \begin{pmatrix} 1 & 0 & 0 \\ m & d & c \\ m_D & b & a \end{pmatrix} \cdot \begin{pmatrix} 1 \\ T \\ T_D \end{pmatrix}$$

  where (m, m_D) are period integrals of C from τ_o to $\frac{d\tau_o - b}{a - c\tau_o}$.

- At large volume $\tau \to \mathrm{i}\infty$, using $C = 1 + \mathcal{O}(q)$ one finds

$$T = \tau + \mathcal{O}(q), \quad T_D = \frac{1}{2}\tau^2 + \frac{1}{8} + \mathcal{O}(q)$$

  in agreement with $Z(\gamma) \sim -\int_S e^{-zH} \operatorname{ch} E \, \mathrm{Td}(S)$.

Space of Bridgeland stability conditions

- Donaldson-Thomas invariants are defined in the larger space of Bridgeland stability conditions Stab $\mathcal{C} = \{\sigma = (Z, \mathcal{A})\}$, where $Z : \Gamma \to \mathbb{C}$ is a linear map and $\mathcal{A} \subset \mathcal{C}$ an Abelian category (heart of t-structure) satisfying various axioms, e.g. $\mathrm{Im} Z(\gamma(E)) \geq 0 \;\forall E \in \mathcal{A}$.

Space of Bridgeland stability conditions

- Donaldson-Thomas invariants are defined in the larger space of Bridgeland stability conditions $\mathrm{Stab}\,\mathcal{C} = \{\sigma = (Z, \mathcal{A})\}$, where $Z : \Gamma \to \mathbb{C}$ is a linear map and $\mathcal{A} \subset \mathcal{C}$ an Abelian category (heart of t-structure) satisfying various axioms, e.g. $\mathrm{Im} Z(\gamma(E)) \geq 0\ \forall E \in \mathcal{A}$.
- The group $\widetilde{GL(2, \mathbb{R})}^+$ acts on $\mathrm{Stab}\,\mathcal{C}$ by linear transformations of $(\mathrm{Re} Z, \mathrm{Im} Z)$ with positive determinant, leaving $\Omega_\sigma(\gamma)$ invariant.

Space of Bridgeland stability conditions

- Donaldson-Thomas invariants are defined in the larger space of Bridgeland stability conditions $\mathrm{Stab}\,\mathcal{C} = \{\sigma = (Z, \mathcal{A})\}$, where $Z : \Gamma \to \mathbb{C}$ is a linear map and $\mathcal{A} \subset \mathcal{C}$ an Abelian category (heart of t-structure) satisfying various axioms, e.g. $\mathrm{Im} Z(\gamma(E)) \geq 0 \; \forall E \in \mathcal{A}$.
- The group $\widetilde{GL(2,\mathbb{R})}^+$ acts on $\mathrm{Stab}\,\mathcal{C}$ by linear transformations of $(\mathrm{Re} Z, \mathrm{Im} Z)$ with positive determinant, leaving $\Omega_\sigma(\gamma)$ invariant.
- For τ_2 large enough, one can use $\widetilde{GL(2,\mathbb{R})}^+$ to absorb the $1/8$ and $\mathcal{O}(q)$ corrections and reach the large volume slice

$$Z^{LV}_{(s,t)}(\gamma) = -\frac{r}{2}(s + \mathrm{i}t)^2 + d(s + \mathrm{i}t) - \mathrm{ch}_2 \,,$$

with $\tau \simeq s + \mathrm{i}t$.

Space of Bridgeland stability conditions

- Specifically, this holds in the region $w > \frac{1}{2}s^2$ where $(s, w) := \left(\frac{\mathrm{Im}\, T_D}{\mathrm{Im}\, T}, -\frac{\mathrm{Im}(T\bar{T}_D)}{\mathrm{Im}\, T}\right)$ and $t = \sqrt{2w - s^2}$.

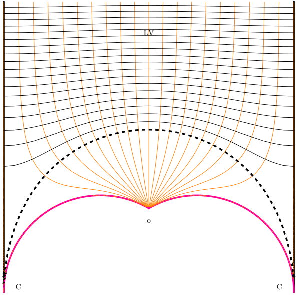

Space of Bridgeland stability conditions

- Specifically, this holds in the region $w > \frac{1}{2}s^2$ where $(s,w) := \left(\frac{\mathrm{Im}\, T_D}{\mathrm{Im}\, T}, -\frac{\mathrm{Im}(T\bar{T}_D)}{\mathrm{Im}\, T}\right)$ and $t = \sqrt{2w - s^2}$.

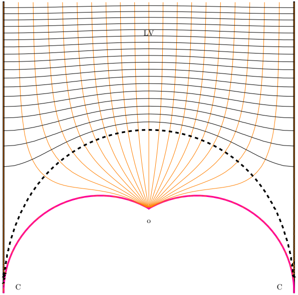

- The large volume slice does not cover the region around the orbifold point, and covers only part of the conifold point.

Outline

Quiver for $K_{\mathbb{P}^2}$

- The category $D^b\,\mathrm{Coh}_c(K_{\mathbb{P}^2})$ is isomorphic to the category of representations a quiver with potential (Q, W), whose nodes correspond to fractional branes on $\mathbb{C}^3/\mathbb{Z}_3$:

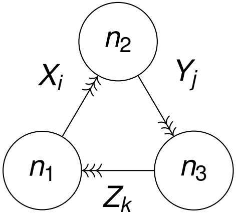

$$W = \sum \epsilon_{ijk} X_i Y_j Z_k$$

$$\begin{aligned} E_1 &= \mathcal{O}[-1] & \gamma_1 &= [-1, 0, 0] \\ E_2 &= \Omega(1), & \gamma_2 &= [2, -1, -\tfrac{1}{2}] \\ E_3 &= \mathcal{O}(-1)[1] & \gamma_3 &= [-1, 1, -\tfrac{1}{2}] \end{aligned}$$

$$\begin{aligned} r &= 2n_2 - n_1 - n_3 \\ d &= n_3 - n_2 \\ \mathrm{ch}_2 &= -\tfrac{1}{2}(n_2 + n_3) \end{aligned}$$

- The quiver description is valid in a region where the central charges $Z(E_i)$ lie in a common half-plane, which includes the orbifold point $\tau_o = -\frac{1}{2} + \frac{\mathrm{i}}{2\sqrt{3}}$, where $Z_{\tau_o}(\gamma_i) = 1/3$ for $i = 1, 2, 3$.

Attractor flow tree formula for quivers

- In that region, $\Omega_\tau(\gamma)$ coincides with the quiver index $\Omega_\theta(\gamma)$ counting θ-semi-stable representations of dimension vector γ, upon setting $\theta_i = -\mathrm{Re}(e^{-\mathrm{i}\psi} Z_\tau(\gamma_i))$ with ψ s.t. $\mathrm{Im}(e^{-\mathrm{i}\psi} Z_\tau(\gamma_i)) > 0$.

Attractor flow tree formula for quivers

- In that region, $\Omega_\tau(\gamma)$ coincides with the quiver index $\Omega_\theta(\gamma)$ counting θ-semi-stable representations of dimension vector γ, upon setting $\theta_i = -\mathrm{Re}(e^{-\mathrm{i}\psi} Z_\tau(\gamma_i))$ with ψ s.t. $\mathrm{Im}(e^{-\mathrm{i}\psi} Z_\tau(\gamma_i)) > 0$.
- For $\theta \in \mathbb{R}^{Q_0}$, θ-semi-stable representations are such that $(\theta, \gamma') \le (\theta, \gamma)$ for any subrepresentation.

Attractor flow tree formula for quivers

- In that region, $\Omega_\tau(\gamma)$ coincides with the quiver index $\Omega_\theta(\gamma)$ counting θ-semi-stable representations of dimension vector γ, upon setting $\theta_i = -\mathrm{Re}(e^{-\mathrm{i}\psi} Z_\tau(\gamma_i))$ with ψ s.t. $\mathrm{Im}(e^{-\mathrm{i}\psi} Z_\tau(\gamma_i)) > 0$.
- For $\theta \in \mathbb{R}^{Q_0}$, θ-semi-stable representations are such that $(\theta, \gamma') \le (\theta, \gamma)$ for any subrepresentation.
- In the quiver context, there is a notion of attractor stability condition (aka self-stability condition)

$$(\theta_\star(\gamma), \gamma') = \langle \gamma', \gamma \rangle := \sum_{a: i \to j} (n'_i n_j - n'_j n_i)$$

The (quiver) attractor invariant is defined as $\Omega_\star(\gamma) := \Omega_{\theta_\star(\gamma)}(\gamma)$

The Flow Tree formula for quivers

- In *[Alexandrov BP'18]*, we conjectured a precise version of SAFC which expresses $\bar{\Omega}_\theta(\gamma)$ in terms of the attractor invariants:

$$\bar{\Omega}_\theta(\gamma) = \sum_{\gamma=\sum \gamma_i} \frac{g_\theta(\{\gamma_i\})}{\mathrm{Aut}(\{\gamma_i\})} \prod_i \bar{\Omega}_\star(\gamma_i)$$

The coefficients $g_\theta(\{\gamma_i\})$ involve a sum over rooted binary trees, whose edges are embedded in $\mathbb{R}^{Q_0}$ along straight lines $\theta_0 + \lambda\theta_\star(\gamma_e)$, which are the analogue of attractor flows.

The Flow Tree formula for quivers

- In *[Alexandrov BP'18]*, we conjectured a precise version of SAFC which expresses $\bar{\Omega}_\theta(\gamma)$ in terms of the attractor invariants:

$$\bar{\Omega}_\theta(\gamma) = \sum_{\gamma=\sum \gamma_i} \frac{g_\theta(\{\gamma_i\})}{\mathrm{Aut}(\{\gamma_i\})} \prod_i \bar{\Omega}_\star(\gamma_i)$$

  The coefficients $g_\theta(\{\gamma_i\})$ involve a sum over rooted binary trees, whose edges are embedded in $\mathbb{R}^{Q_0}$ along straight lines $\theta_0 + \lambda\theta_\star(\gamma_e)$, which are the analogue of attractor flows.
- The sum is manifestly finite, since γ_i lie in the positive cone $\mathbb{Z}_+^{Q_0}$.

The Flow Tree formula for quivers

- In *[Alexandrov BP'18]*, we conjectured a precise version of SAFC which expresses $\bar{\Omega}_\theta(\gamma)$ in terms of the attractor invariants:

$$\bar{\Omega}_\theta(\gamma) = \sum_{\gamma=\sum \gamma_i} \frac{g_\theta(\{\gamma_i\})}{\mathrm{Aut}(\{\gamma_i\})} \prod_i \bar{\Omega}_\star(\gamma_i)$$

  The coefficients $g_\theta(\{\gamma_i\})$ involve a sum over rooted binary trees, whose edges are embedded in $\mathbb{R}^{Q_0}$ along straight lines $\theta_0 + \lambda \theta_\star(\gamma_e)$, which are the analogue of attractor flows.
- The sum is manifestly finite, since γ_i lie in the positive cone $\mathbb{Z}_+^{Q_0}$.
- The formula was proven mathematically in *[Argüz Bousseau'21]* using the formalism of scattering diagrams.

Flow tree formula from scattering diagrams

- For any quiver with potential (Q, W), the scattering diagram $\mathcal{D}_Q$ is the set of real codimension-one rays $\{\mathcal{R}(\gamma), \gamma \in \mathbb{Z}^{Q_0}\}$ defined by

$$\mathcal{R}(\gamma) = \{\theta \in \mathbb{R}^{Q_0} : (\theta, \gamma) = 0,\ \bar{\Omega}_\theta(\gamma) \neq 0\}$$

Flow tree formula from scattering diagrams

- For any quiver with potential (Q, W), the scattering diagram $\mathcal{D}_Q$ is the set of real codimension-one rays $\{\mathcal{R}(\gamma), \gamma \in \mathbb{Z}^{Q_0}\}$ defined by

$$\mathcal{R}(\gamma) = \{\theta \in \mathbb{R}^{Q_0} : (\theta, \gamma) = 0,\ \bar{\Omega}_\theta(\gamma) \neq 0\}$$

- Each point along $\mathcal{R}(\gamma)$ is endowed with an automorphism of the quantum torus algebra,

$$\mathcal{U}_\theta(\gamma) = \exp\left(\frac{\bar{\Omega}_\theta(\gamma)}{y^{-1} - y}\mathcal{X}_\gamma\right) \ , \quad \mathcal{X}_\gamma \mathcal{X}_{\gamma'} = (-y)^{\langle\gamma,\gamma'\rangle}\mathcal{X}_{\gamma+\gamma'}$$

Flow tree formula from scattering diagrams

- For any quiver with potential (Q, W), the scattering diagram $\mathcal{D}_Q$ is the set of real codimension-one rays $\{\mathcal{R}(\gamma), \gamma \in \mathbb{Z}^{Q_0}\}$ defined by

$$\mathcal{R}(\gamma) = \{\theta \in \mathbb{R}^{Q_0} : (\theta, \gamma) = 0,\ \bar{\Omega}_\theta(\gamma) \neq 0\}$$

- Each point along $\mathcal{R}(\gamma)$ is endowed with an automorphism of the quantum torus algebra,

$$\mathcal{U}_\theta(\gamma) = \exp\left(\frac{\bar{\Omega}_\theta(\gamma)}{y^{-1} - y} \mathcal{X}_\gamma\right) \ , \quad \mathcal{X}_\gamma \mathcal{X}_{\gamma'} = (-y)^{\langle \gamma, \gamma' \rangle} \mathcal{X}_{\gamma+\gamma'}$$

- The WCF ensures that the diagram is consistent: for any generic closed path $\mathcal{P} : t \in [0,1] \in \mathbb{R}^{Q_0}$, $\prod_i \mathcal{U}_{\theta(t_i)}(\gamma_i)^{\epsilon_i} = 1$ *[Bridgeland'16]*

Flow tree formula from scattering diagrams

- For any quiver with potential (Q, W), the scattering diagram $\mathcal{D}_Q$ is the set of real codimension-one rays $\{\mathcal{R}(\gamma), \gamma \in \mathbb{Z}^{Q_0}\}$ defined by

$$\mathcal{R}(\gamma) = \{\theta \in \mathbb{R}^{Q_0} : (\theta, \gamma) = 0,\ \bar{\Omega}_\theta(\gamma) \neq 0\}$$

- Each point along $\mathcal{R}(\gamma)$ is endowed with an automorphism of the quantum torus algebra,

$$\mathcal{U}_\theta(\gamma) = \exp\left(\frac{\bar{\Omega}_\theta(\gamma)}{y^{-1}-y}\mathcal{X}_\gamma\right) \quad , \quad \mathcal{X}_\gamma \mathcal{X}_{\gamma'} = (-y)^{\langle\gamma,\gamma'\rangle}\mathcal{X}_{\gamma+\gamma'}$$

- The WCF ensures that the diagram is consistent: for any generic closed path $\mathcal{P} : t \in [0,1] \in \mathbb{R}^{Q_0}$, $\prod_i \mathcal{U}_{\theta(t_i)}(\gamma_i)^{\epsilon_i} = 1$ *[Bridgeland'16]*
- A consistent scattering diagram is uniquely determined from the initial rays $\mathcal{R}_\star(\gamma)$, defined as those which contain $\theta_\star(\gamma)$.

Flow tree formula from scattering diagrams

- For any quiver with potential (Q, W), the scattering diagram $\mathcal{D}_Q$ is the set of real codimension-one rays $\{\mathcal{R}(\gamma), \gamma \in \mathbb{Z}^{Q_0}\}$ defined by

$$\mathcal{R}(\gamma) = \{\theta \in \mathbb{R}^{Q_0} : (\theta, \gamma) = 0,\ \bar{\Omega}_\theta(\gamma) \neq 0\}$$

- Each point along $\mathcal{R}(\gamma)$ is endowed with an automorphism of the quantum torus algebra,

$$\mathcal{U}_\theta(\gamma) = \exp\left(\frac{\bar{\Omega}_\theta(\gamma)}{y^{-1} - y} \mathcal{X}_\gamma\right) \ , \quad \mathcal{X}_\gamma \mathcal{X}_{\gamma'} = (-y)^{\langle \gamma, \gamma' \rangle} \mathcal{X}_{\gamma+\gamma'}$$

- The WCF ensures that the diagram is consistent: for any generic closed path $\mathcal{P} : t \in [0, 1] \in \mathbb{R}^{Q_0}$, $\prod_i \mathcal{U}_{\theta(t_i)}(\gamma_i)^{\epsilon_i} = 1$ *[Bridgeland'16]*
- A consistent scattering diagram is uniquely determined from the initial rays $\mathcal{R}_\star(\gamma)$, defined as those which contain $\theta_\star(\gamma)$.
- The Flow Tree Formula of *[Alexandrov BP'18]* determines the indices of outgoing rays produced by scattering initial rays *[Argüz Bousseau '20]*.

Scattering diagram for Kronecker quiver

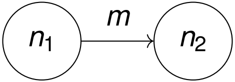

$$\theta_1 > 0, \theta_2 < 0 : \quad \dim \mathcal{M}_\theta(\gamma) = m n_1 n_2 - n_1^2 - n_2^2 + 1$$

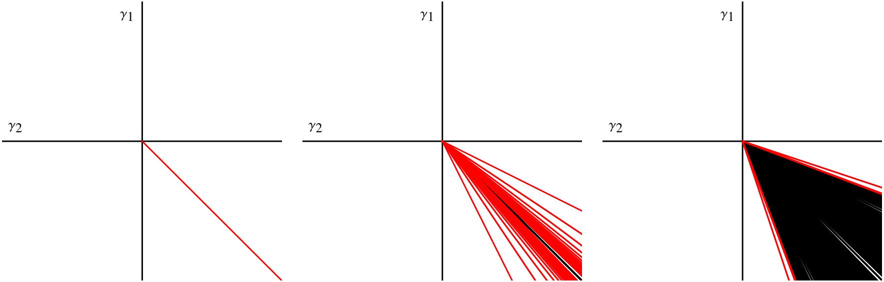

m=1 m=2 m=3

Attractor conjecture for $K_{\mathbb{P}^2}$

- By studying expected dimension of $\mathcal{M}_\theta(\gamma)$ for the orbifold quiver, *[Beaujard BP Manschot'20]* conjectured that the attractor index $\Omega_\star(\gamma)$ vanishes unless for $\gamma = \gamma_i$ or $\gamma = k(\gamma_1 + \gamma_2 + \gamma_3)$. This is now a theorem.

Attractor conjecture for $K_{\mathbb{P}^2}$

- By studying expected dimension of $\mathcal{M}_\theta(\gamma)$ for the orbifold quiver, *[Beaujard BP Manschot'20]* conjectured that the attractor index $\Omega_\star(\gamma)$ vanishes unless for $\gamma = \gamma_i$ or $\gamma = k(\gamma_1 + \gamma_2 + \gamma_3)$. This is now a theorem.

Attractor conjecture for $K_{\mathbb{P}^2}$

- By studying expected dimension of $\mathcal{M}_\theta(\gamma)$ for the orbifold quiver, *[Beaujard BP Manschot'20]* conjectured that the attractor index $\Omega_\star(\gamma)$ vanishes unless for $\gamma = \gamma_i$ or $\gamma = k(\gamma_1 + \gamma_2 + \gamma_3)$. This is now a theorem.

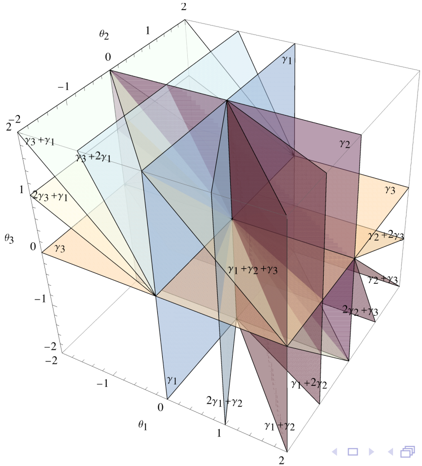

A 2D slice of the orbifold scattering diagram

Let $\mathcal{D}_o$ be the restriction of $\mathcal{D}_Q$ to the hyperplane $\theta_1 + \theta_2 + \theta_3 = 1$:

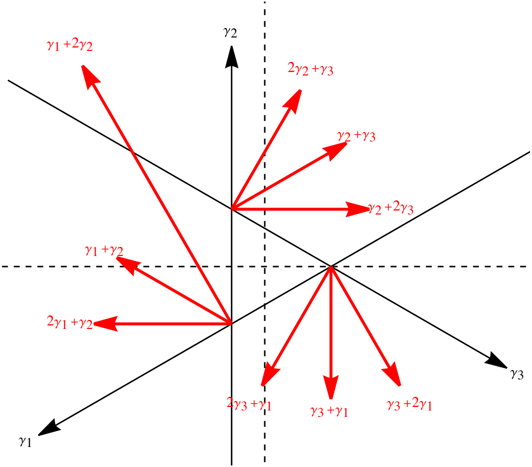

A 2D slice of the orbifold scattering diagram

Let $\mathcal{D}_o$ be the restriction of $\mathcal{D}_Q$ to the hyperplane $\theta_1 + \theta_2 + \theta_3 = 1$:

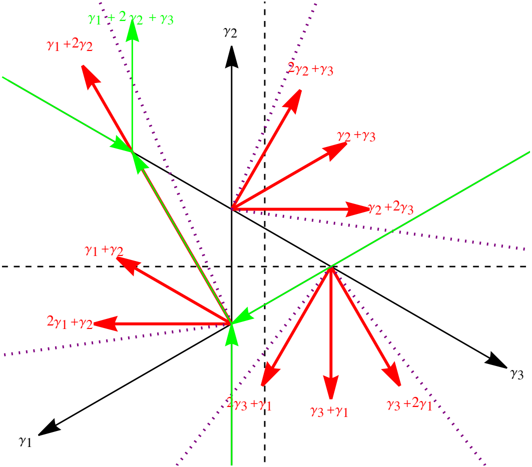

A 2D slice of the orbifold scattering diagram

The full scattering diagram $\mathcal{D}_Q$ includes regions with dense set of rays:

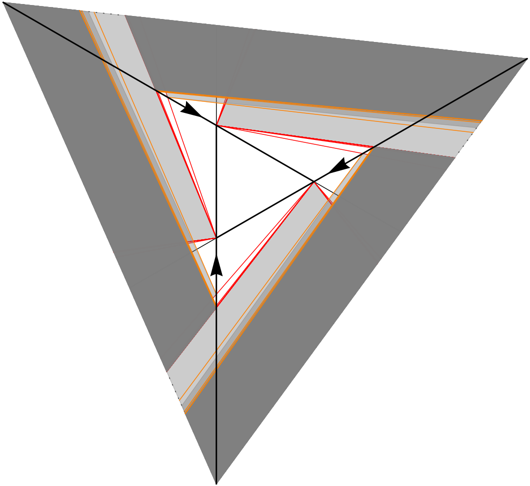

Scattering diagrams on triangulated categories

- For a general triangulated category $\mathcal{C}$, define the scattering diagram $\mathcal{D}_\psi(\mathcal{C})$ as the set of codimension-one loci in Stab $\mathcal{C}$,

$$\mathcal{R}_\psi(\gamma) = \{\sigma : \arg Z(\gamma) = \psi + \tfrac{\pi}{2},\ \bar{\Omega}_Z(\gamma) \neq 0\}$$

equipped with (a suitable regularization of) the automorphism

$$\mathcal{U}_\sigma(\gamma) = \exp\left(\frac{\bar{\Omega}_\sigma(\gamma)}{y^{-1} - y} \mathcal{X}_\gamma\right)$$

Scattering diagrams on triangulated categories

- For a general triangulated category $\mathcal{C}$, define the scattering diagram $\mathcal{D}_\psi(\mathcal{C})$ as the set of codimension-one loci in Stab $\mathcal{C}$,

$$\mathcal{R}_\psi(\gamma) = \{\sigma : \arg Z(\gamma) = \psi + \tfrac{\pi}{2},\ \bar{\Omega}_Z(\gamma) \neq 0\}$$

equipped with (a suitable regularization of) the automorphism

$$\mathcal{U}_\sigma(\gamma) = \exp\left(\frac{\bar{\Omega}_\sigma(\gamma)}{y^{-1}-y}\mathcal{X}_\gamma\right)$$

- The WCF ensures that the diagram $\mathcal{D}_\psi$ is still locally consistent at each codimension-two intersection.

Flow trees from scattering diagrams

- To see the relation to SAFC, note that for any local CY threefold, the central charge $Z_z(\gamma)$ is holomorphic in z^a, hence its argument is constant along $\frac{\mathrm{d}z^a}{\mathrm{d}\mu} = -g^{a\bar{b}}\partial_{\bar{b}}|Z_z(\gamma)|^2$:

$$\frac{1}{2}\frac{\mathrm{d}}{\mathrm{d}\mu}\log\frac{Z(\gamma)}{\bar{Z}(\gamma)} = -\frac{1}{2}\partial_a Z(\gamma)g^{a\bar{b}}\partial_{\bar{b}}\bar{Z}(\gamma) + \frac{1}{2}\partial_a Z(\gamma)g^{a\bar{b}}\partial_{\bar{b}}\bar{Z}(\gamma) = 0$$

Moreover, $|Z_z(\gamma)|^2$ has no local minima so the only attractor points are conifold points with $Z_z(\gamma_i) = 0$.

Flow trees from scattering diagrams

- To see the relation to SAFC, note that for any local CY threefold, the central charge $Z_z(\gamma)$ is holomorphic in z^a, hence its argument is constant along $\frac{\mathrm{d}z^a}{\mathrm{d}\mu} = -g^{a\bar{b}}\partial_{\bar{b}}|Z_z(\gamma)|^2$:

$$\frac{1}{2}\frac{\mathrm{d}}{\mathrm{d}\mu}\log\frac{Z(\gamma)}{\bar{Z}(\gamma)} = -\frac{1}{2}\partial_a Z(\gamma) g^{a\bar{b}}\partial_{\bar{b}}\bar{Z}(\gamma) + \frac{1}{2}\partial_a Z(\gamma) g^{a\bar{b}}\partial_{\bar{b}}\bar{Z}(\gamma) = 0$$

  Moreover, $|Z_z(\gamma)|^2$ has no local minima so the only attractor points are conifold points with $Z_z(\gamma_i) = 0$.
- Thus, the restriction of $\mathcal{R}_\psi(\gamma)$ to the physical slice is preserved by the attractor flow. Moreover, the flow can only split when $\mathcal{R}(\gamma_L)$ and $\mathcal{R}(\gamma_R)$ intersect, and end on an initial ray $\mathcal{R}_\psi(\gamma_i)$.

Flow trees from scattering diagrams

- To see the relation to SAFC, note that for any local CY threefold, the central charge $Z_z(\gamma)$ is holomorphic in z^a, hence its argument is constant along $\frac{\mathrm{d}z^a}{\mathrm{d}\mu} = -g^{a\bar{b}}\partial_{\bar{b}}|Z_z(\gamma)|^2$:

$$\frac{1}{2}\frac{\mathrm{d}}{\mathrm{d}\mu}\log\frac{Z(\gamma)}{\bar{Z}(\gamma)} = -\frac{1}{2}\partial_a Z(\gamma) g^{a\bar{b}}\partial_{\bar{b}}\bar{Z}(\gamma) + \frac{1}{2}\partial_a Z(\gamma) g^{a\bar{b}}\partial_{\bar{b}}\bar{Z}(\gamma) = 0$$

  Moreover, $|Z_z(\gamma)|^2$ has no local minima so the only attractor points are conifold points with $Z_z(\gamma_i) = 0$.
- Thus, the restriction of $\mathcal{R}_\psi(\gamma)$ to the physical slice is preserved by the attractor flow. Moreover, the flow can only split when $\mathcal{R}(\gamma_L)$ and $\mathcal{R}(\gamma_R)$ intersect, and end on an initial ray $\mathcal{R}_\psi(\gamma_i)$.
- In complex dimension one, attractor flow lines and scattering rays coincide. Attractor flow trees are subsets of $\mathcal{D}_\psi$ which produce an outgoing ray $\mathcal{R}_\psi(\gamma)$ with desired charge γ, passing through the desired point z.

Outline

Large volume scattering diagram

- The scattering diagram $\mathcal{D}_{\psi}^{\rm LV}$ along the large volume slice

$$Z_{(s,t)}^{LV} = -\frac{1}{2} r(s+\mathrm{i}t)^2 + d(s+\mathrm{i}t) - \mathrm{ch}_2$$

was determined for $\psi = 0$ in *[Bousseau'19]*, using a different set of coordinates. The construction extends to any ψ by just mapping $(s,t) \mapsto (s - t\tan\psi, t/\cos\psi)$.

Large volume scattering diagram

- The scattering diagram $\mathcal{D}_\psi^{\rm LV}$ along the large volume slice

$$Z^{LV}_{(s,t)} = -\frac{1}{2} r(s+\mathrm{i}t)^2 + d(s+\mathrm{i}t) - \mathrm{ch}_2$$

  was determined for $\psi = 0$ in *[Bousseau'19]*, using a different set of coordinates. The construction extends to any ψ by just mapping $(s,t) \mapsto (s - t\tan\psi, t/\cos\psi)$.
- Since $\mathrm{Re} Z(\gamma) = \frac{1}{2} r(t^2 - s^2) + ds - \mathrm{ch}_2$, each ray $\mathcal{R}_0(\gamma)$ is contained in a branch of hyperbola asymptoting to $t = \pm(s - \frac{d}{r})$ for $r \neq 0$, or vertical a line when $r = 0$. Walls of marginal stability $\mathcal{W}(\gamma, \gamma')$ are half-circles centered on real axis.

Large volume scattering diagram

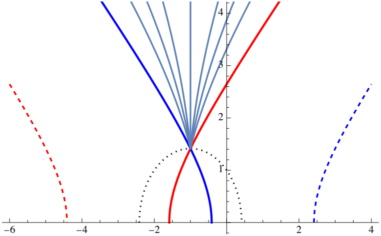

It is useful to think of $\mathcal{R}(\gamma)$ as the worldline of a fictitious particle of charge r, mass $M^2 = \frac{1}{2}d^2 - r\,\mathrm{ch}_2$ moving in a constant electric field:

- The particle travels inside the forward light-cone

Large volume scattering diagram

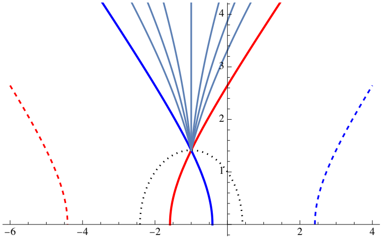

It is useful to think of $\mathcal{R}(\gamma)$ as the worldline of a fictitious particle of charge r, mass $M^2 = \frac{1}{2}d^2 - r\,\mathrm{ch}_2$ moving in a constant electric field:

- The particle travels inside the forward light-cone
- the 'electric potential' $\varphi_s(\gamma) = 2(d - sr) = 2\mathrm{Im}Z_\gamma/t$ increases along the flow.

Large volume scattering diagram

- Initial rays correspond to $\mathcal{O}(m)$ and $\mathcal{O}(m)[1]$, with charge $\gamma_m = \pm[1, m, \frac{1}{2}m^2]$, emanating from $(s,t) = (m,0)$ on the boundary where $Z^{LV}_{(s,t)}(\gamma_m) = 0$. *[Bousseau'19]*

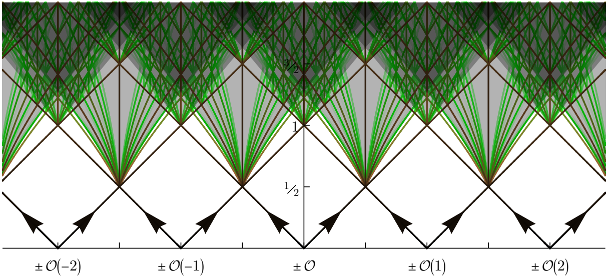

Large volume scattering diagram

- Initial rays correspond to $\mathcal{O}(m)$ and $\mathcal{O}(m)[1]$, with charge $\gamma_m = \pm[1, m, \frac{1}{2}m^2]$, emanating from $(s,t) = (m,0)$ on the boundary where $Z^{LV}_{(s,t)}(\gamma_m) = 0$. *[Bousseau'19]*

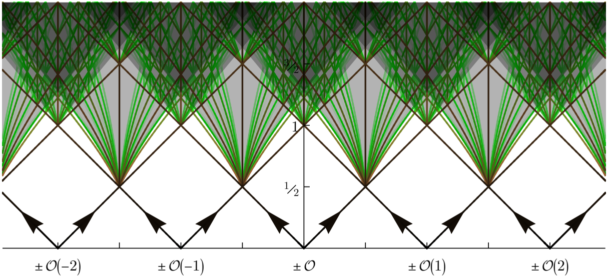

- Physically, the BPS spectrum along the large volume slice originates from bound states of fluxed D4-branes and anti-D4 branes.

SAFC holds along large volume slice

- The first scatterings occur after a time $t \geq \frac{1}{2}$, after each constituent $k_i\mathcal{O}(m_i)$ has moved by $|\Delta s| \geq \frac{1}{2}$, by which time $\varphi_s(\gamma_i) \geq |k_i|$.

SAFC holds along large volume slice

- The first scatterings occur after a time $t \geq \frac{1}{2}$, after each constituent $k_i \mathcal{O}(m_i)$ has moved by $|\Delta s| \geq \frac{1}{2}$, by which time $\varphi_s(\gamma_i) \geq |k_i|$.
- Since $\varphi_s(\gamma)$ is additive at each vertex, this allows to bound the number and charges of constituents contributing to $\Omega_{(s,t)}(\gamma)$:

$$\sum_i k_i [1, m_i, \frac{1}{2} m_i^2] = \gamma \ , \quad s - t \leq m_i \leq s + t, \quad \sum |k_i| \leq \varphi_s(\gamma)$$

SAFC holds along large volume slice

- The first scatterings occur after a time $t \geq \frac{1}{2}$, after each constituent $k_i \mathcal{O}(m_i)$ has moved by $|\Delta s| \geq \frac{1}{2}$, by which time $\varphi_s(\gamma_i) \geq |k_i|$.
- Since $\varphi_s(\gamma)$ is additive at each vertex, this allows to bound the number and charges of constituents contributing to $\Omega_{(s,t)}(\gamma)$:

$$\sum_i k_i[1, m_i, \frac{1}{2} m_i^2] = \gamma \ , \quad s - t \leq m_i \leq s + t, \quad \sum |k_i| \leq \varphi_s(\gamma)$$

- Thus, SAFC holds along the large volume slice !

Flow trees for $\gamma = [0, 4, 1)$

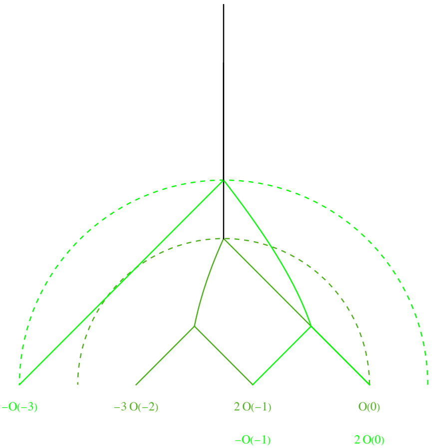

- $\{\{-3\mathcal{O}(-2), 2\mathcal{O}(-1)\}, \mathcal{O}\}$:
  $3\mathcal{O}(-2) \to 2\mathcal{O}(-1) \oplus \mathcal{O} \to E$
  $K_3(2,3)K_{12}(1,1) \to -156$
- $\{-\mathcal{O}(-3), \{-\mathcal{O}(-1), 2\mathcal{O}\}\}$:
  $\mathcal{O}(-3) \oplus \mathcal{O}(-1) \to 2\mathcal{O} \to E$
  $K_3(1,2)K_{12}(1,1) \to -36$

Total: $\Omega_\infty(\gamma) = -192 = GV_4^{(0)}$

Flow trees for $\gamma = [1, 0, -3)$

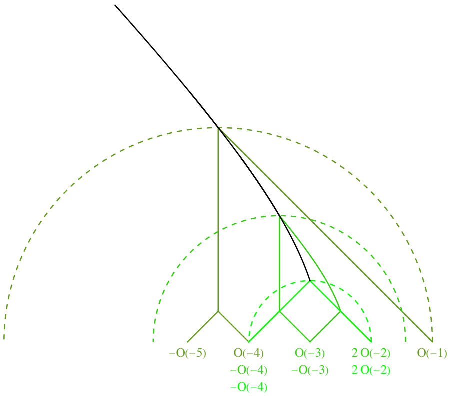

- $\{\{-\mathcal{O}(-5), \mathcal{O}(-4)\}, \mathcal{O}(-1)\}$
  $\mathcal{O}(-5) \to \mathcal{O}(-4) \oplus \mathcal{O}(-1) \to E$
  $K_3(1,1)^2 \to 9$
- $\{\{-\mathcal{O}(-4), \mathcal{O}(-3)\},$
  $\{-\mathcal{O}(-3), 2\mathcal{O}(-2)\}\}$
  $\mathcal{O}(-4) \oplus \mathcal{O}(-3) \to$
  $\mathcal{O}(-3) \oplus 2\mathcal{O}(-2) \to E$
  $K_3(1,1)^2 K_3(1,2) \to 27$
- $\{-\mathcal{O}(-4), 2\mathcal{O}(-2)\}$
  $\mathcal{O}(-4) \to 2\mathcal{O}(-2) \to E$
  $K_6(1,2) \to 15$

Total: $\Omega_\infty(\gamma) = 51 = \chi(\mathrm{Hilb}_4 \mathbb{P}^2)$

Outline

Exact scattering diagram

- The scattering diagram $\mathcal{D}_\psi^\Pi$ along the physical slice should interpolate between $\mathcal{D}_\psi^{\rm LV}$ around $\tau = \mathrm{i}\infty$ and $\mathcal{D}_o$ around $\tau = \tau_o$, and be invariant under the action of $\Gamma_1(3)$.

Exact scattering diagram

- The scattering diagram $\mathcal{D}^{\Pi}_{\psi}$ along the physical slice should interpolate between $\mathcal{D}^{\rm LV}_{\psi}$ around $\tau = {\rm i}\infty$ and $\mathcal{D}_o$ around $\tau = \tau_o$, and be invariant under the action of $\Gamma_1(3)$.
- Under $\tau \mapsto \frac{\tau}{3n\tau+1}$ with $n \in \mathbb{Z}$, $\mathcal{O} \mapsto \mathcal{O}[n]$. Hence there is a doubly infinite family of initial rays emitted at $\tau = 0$, associated to $\mathcal{O}[n]$.

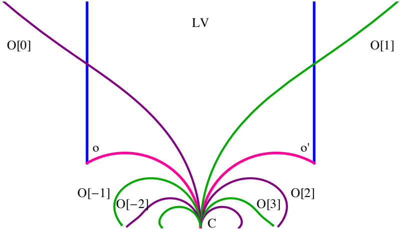

Exact scattering diagram

- The scattering diagram $\mathcal{D}_\psi^\Pi$ along the physical slice should interpolate between $\mathcal{D}_\psi^{\rm LV}$ around $\tau = \mathrm{i}\infty$ and $\mathcal{D}_o$ around $\tau = \tau_o$, and be invariant under the action of $\Gamma_1(3)$.
- Under $\tau \mapsto \frac{\tau}{3n\tau+1}$ with $n \in \mathbb{Z}$, $\mathcal{O} \mapsto \mathcal{O}[n]$. Hence there is a doubly infinite family of initial rays emitted at $\tau = 0$, associated to $\mathcal{O}[n]$.

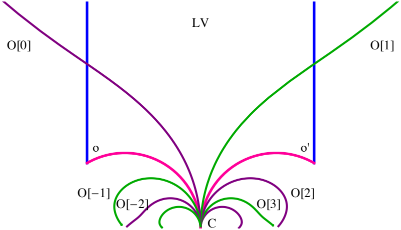

- Similarly, there must be an infinite family of initial rays coming from $\tau = \frac{p}{q}$ with $q \neq 0 \mod 3$, corresponding to $\Gamma_1(3)$-images of $\mathcal{O}[n]$. In particular, from the conifold points $\tau = 0, 1/2, 1$, where the objects E_i in the orbifold quiver become massless.

Exact scattering diagram for small ψ

- For $|\psi|$ small enough, the only rays which reach the large volume region are those associated to $\mathcal{O}(m)$ and $\mathcal{O}(m)[1]$. Thus, the scattering diagram $\mathcal{D}_\psi^\Pi$ is isomorphic to $\mathcal{D}_0^{\mathrm{LV}}$ inside $\mathcal{F}$ and its translates:

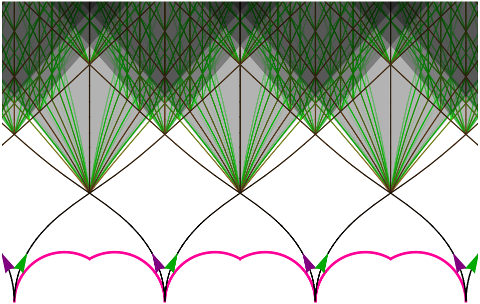

Exact scattering diagram for $\psi = \pm\frac{\pi}{2}$

- For $\psi = \pm\frac{\pi}{2}$, the geometric rays $\{\mathrm{Im} Z_\tau(\gamma) = 0\}$ coincide with lines of constant $s = \frac{\mathrm{Im}\, T_D}{\mathrm{Im}\, T} = \frac{d}{r}$, independent of ch_2:

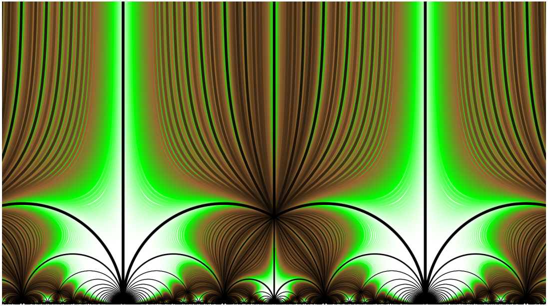

Exact scattering diagram for $\psi = \pm\frac{\pi}{2}$

- For $\psi = \pm\frac{\pi}{2}$, the geometric rays $\{\mathrm{Im} Z_\tau(\gamma) = 0\}$ coincide with lines of constant $s = \frac{\mathrm{Im}\, T_D}{\mathrm{Im}\, T} = \frac{d}{r}$, independent of ch_2:

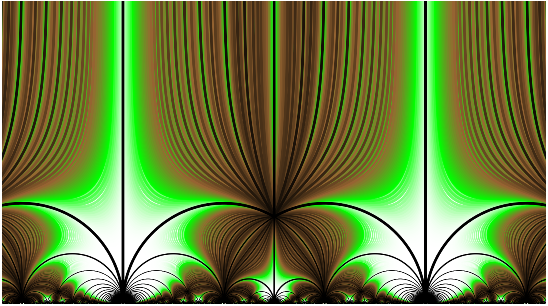

- Hence, there is no wall-crossing between τ_o and $\tau = \mathrm{i}\infty$ when $-1 \leq \frac{d}{r} \leq 0$, explaining why the Gieseker index $\Omega_\infty(\gamma)$ agrees with the quiver index $\Omega_c(\gamma)$ in the anti-attractor chamber.

Douglas Fiol Romelsberger'00, Beaujard BP Manschot'20

Exact scattering diagram, $\mathcal{V}_\psi = 1/2$

As $|\psi|$ reaches a critical value $\simeq .082406$, the topology changes, as the rays $\mathcal{R}_\psi(\mathcal{O}(m)[1]))$ end up at the conifold point $\tau = m + 1$ rather than $\tau = \mathrm{i}\infty$.

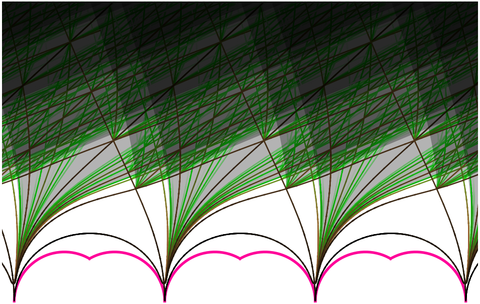

Critical phases for the exact scattering diagram

- More generally, let $\mathcal{V}_\psi = \mathcal{V} \tan \psi$ where $\mathcal{V}$ is the quantum volume

$$\mathcal{V} = \mathrm{Im}\, T(0) = \frac{27}{4\pi^2} \mathrm{Im}\mathrm{Li}_2(e^{2\pi \mathrm{i}/3}) \simeq 0.463$$

Critical phases for the exact scattering diagram

- More generally, let $\mathcal{V}_\psi = \mathcal{V} \tan\psi$ where $\mathcal{V}$ is the quantum volume

$$\mathcal{V} = \mathrm{Im}\, T(0) = \frac{27}{4\pi^2} \mathrm{Im} \mathrm{Li}_2(e^{2\pi \mathrm{i}/3}) \simeq 0.463$$

- The topology of $\mathcal{D}_\psi^\Pi$ jumps at a discrete set of rational values

$$\mathcal{V}_\psi \in \{ \frac{F_{2k} + F_{2k+2}}{2F_{2k+1}}, k \geq 0 \} = \{ \tfrac12, 1, \tfrac{11}{10}, \tfrac{29}{26}, \tfrac{19}{17}, \dots \}$$

and a dense set of values in $[\frac{\sqrt{5}}{2}, +\infty)$ where secondary rays pass through a conifold point.

Case studies

$\gamma = [0, 1, 1) = \text{ch}\, \mathcal{O}_C$:

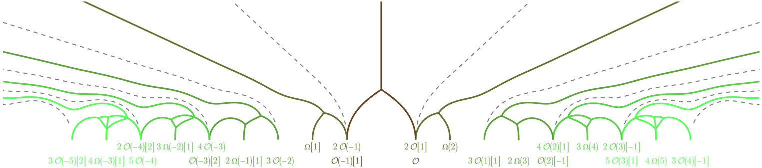

$\gamma = [1, 0, 1) = \text{ch}\, \mathcal{O}$:

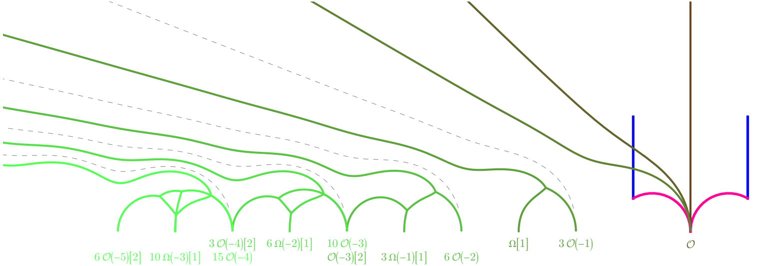

SAFC along the physical slice

- In general, trees reaching the large volume region have a two-stage structure, with initial rays from a finite set of exceptional collections $\{E_1(m_i), E_2(m_i), E_3(m_i)\}$, which scatter in the vicinity of orbifold points $\tau = \tau_o + m_i$, and then further interact in the large volume region.

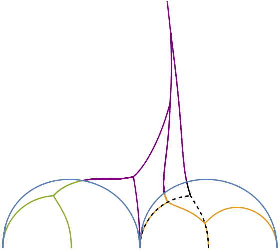

SAFC along the physical slice

- In general, trees reaching the large volume region have a two-stage structure, with initial rays from a finite set of exceptional collections $\{E_1(m_i), E_2(m_i), E_3(m_i)\}$, which scatter in the vicinity of orbifold points $\tau = \tau_o + m_i$, and then further interact in the large volume region.

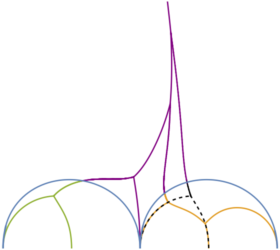

- The full proof of SFAC along physical slice will appear ‘soon’.

Conclusion - outlook

- The scattering diagram is the proper mathematical framework for the attractor flow tree formula in the case of local CY3. This is because $Z(\gamma)$ is holomorphic on $\mathcal{M}_K$, so the gradient flow preserves $\arg Z(\gamma)$.

Conclusion - outlook

- The scattering diagram is the proper mathematical framework for the attractor flow tree formula in the case of local CY3. This is because $Z(\gamma)$ is holomorphic on $\mathcal{M}_K$, so the gradient flow preserves $\arg Z(\gamma)$.
- This provides an effective way of computing (unframed) BPS invariants in any chamber, and a natural decomposition into elementary constituents. Is this mathematically meaningful ? Does it help e.g. in understanding modularity ?

Conclusion - outlook

- The scattering diagram is the proper mathematical framework for the attractor flow tree formula in the case of local CY3. This is because $Z(\gamma)$ is holomorphic on $\mathcal{M}_K$, so the gradient flow preserves $\arg Z(\gamma)$.
- This provides an effective way of computing (unframed) BPS invariants in any chamber, and a natural decomposition into elementary constituents. Is this mathematically meaningful ? Does it help e.g. in understanding modularity ?
- It would be interesting to extend this description to other toric CY3, such as local del Pezzo surfaces.

Conclusion - outlook

- The scattering diagram is the proper mathematical framework for the attractor flow tree formula in the case of local CY3. This is because $Z(\gamma)$ is holomorphic on $\mathcal{M}_K$, so the gradient flow preserves $\arg Z(\gamma)$.
- This provides an effective way of computing (unframed) BPS invariants in any chamber, and a natural decomposition into elementary constituents. Is this mathematically meaningful ? Does it help e.g. in understanding modularity ?
- It would be interesting to extend this description to other toric CY3, such as local del Pezzo surfaces.
- For compact CY3, $Z(\gamma) = e^{K/2} Z_{\rm hol}(\gamma)$ is not longer holomorphic, so $\arg Z(\gamma)$ is not constant along the flow. Can scattering diagrams on Stab $\mathcal{C}$ still be useful in that context ?

Thanks for your attention !